International Geology Review, Vol. 46, 2004, p. 655–670.
Copyright © 2004 by V. H. Winston & Son, Inc. All rights reserved.

The Deep Resistivity Structure of Southwestern Turkey: Tectonic Implications

AYSAN GÜRER,[1] MURAT BAYRAK,

Istanbul University, Engineering Faculty, Geophysical Engineering Department, Avcilar, 34850 Istanbul, Turkey

Ö. FEYZI GÜRER,

Kocaeli University, Engineering Faculty, Geological Engineering Department, Kocaeli, Turkey

O. METIN ILKIŞIK

Anadolu Yerbilimleri, Perpa-A, 5th Floor, No: 152, Sisli, Istanbul, Turkey

Abstract

Magnetotelluric data along two profiles, across the Lycian nappes and the Beydag autochthon of the southwestern Taurides in the eastern Mediterranean region images shallow and deep crustal structures. Inversion of the magnetotelluric data from profiles K and H reveals two subzones of the crust of varying thickness; the first is the conductive and viscoelastic lower crust (< 75 ohm m), whereas the second is the resistive (500–7500 ohm m) and brittle upper crust. The thickness of the uppermost conductive units, the Lycian nappes, is found to be 3.5–4 km in the northwest and 0.5 km in the southeast. The total thickness of the autochthon that forms the resistive upper crust varies from 7–16 km beneath the Lycian nappes to 11–20 km beneath the Korkuteli region along profile K. The depth to the upper/lower crust boundary varies from 10 to 30 km in the region. The resistive upper crust is interrupted by more conductive vertical zones. One of these zones along profile K coincides with the Fethiye Burdur fault zone (FBFZ), one of the most prominent geological structures in the region. The FBFZ lies in continuity with the Pliny and the Strabo subduction zones in the Mediterranean Sea. Projections of all the vertical resistivity discontinuities in the MT images onto the gravity map with the main surface faults show an alignment parallel to the FBFZ, and the Pliny and the Strabo trenches. The Bouguer gravity map shows a low gravity zone between the towns of Fethiye and Burdur. This gravity low also coincides with the alignment of projections of vertical high conductivity zones onto the map. Almost no earthquakes occur in the conductive lower crust, whereas significant earthquakes occur in the resistive upper crust, and the resistive lithospheric upper mantle (~250 ohm m) in the southeastern part of the region along the profile K. In contrast, in the northwestern part of the profile, the upper mantle is conductive (80 ohm m), indicating a viscoelastic character.

Introduction

THE STUDY AREA IS LOCATED at the junction of the eastern Mediterranean region that marks a seismically active part of the broad transition zone between the African and Eurasian plates. Prominent active tectonic elements in the region are shown in Figure 1A. The African plate descends northward beneath the Aegean and Anatolian microplates, and convergence between the African and Anatolian microplates takes place by subduction along the Aegean and Cyprus arcs as shown in Figure 1A (McKenzie, 1978). Several trenches have been distinguished along the eastern parts of the Aegean arc. As a result of subduction in the eastern Aegean arc, compressional motion along these trenches is transformed to slip motion by the Pliny and the Strabo strike-slip faults through southwestern Anatolia. On the land side in southwest Anatolia, the Fethiye–Burdur fault zone (FBFZ) is one of the most striking tectonic elements. Along the FBFZ, normal faulting is distributed with a strongly pronounced lateral strike-slip component (Taymaz and Price, 1992; Temiz et. al., 1997; Koçyigit, 2000; Yagmurlu, 2000). The FBFZ lies in continuity with the Pliny fault zone on the land side (southwest Turkey); this is thought to be the border between the west and central Anatolian blocks, which are under extensional and

[1]Corresponding author; email: agurer@istanbul.tr.edu

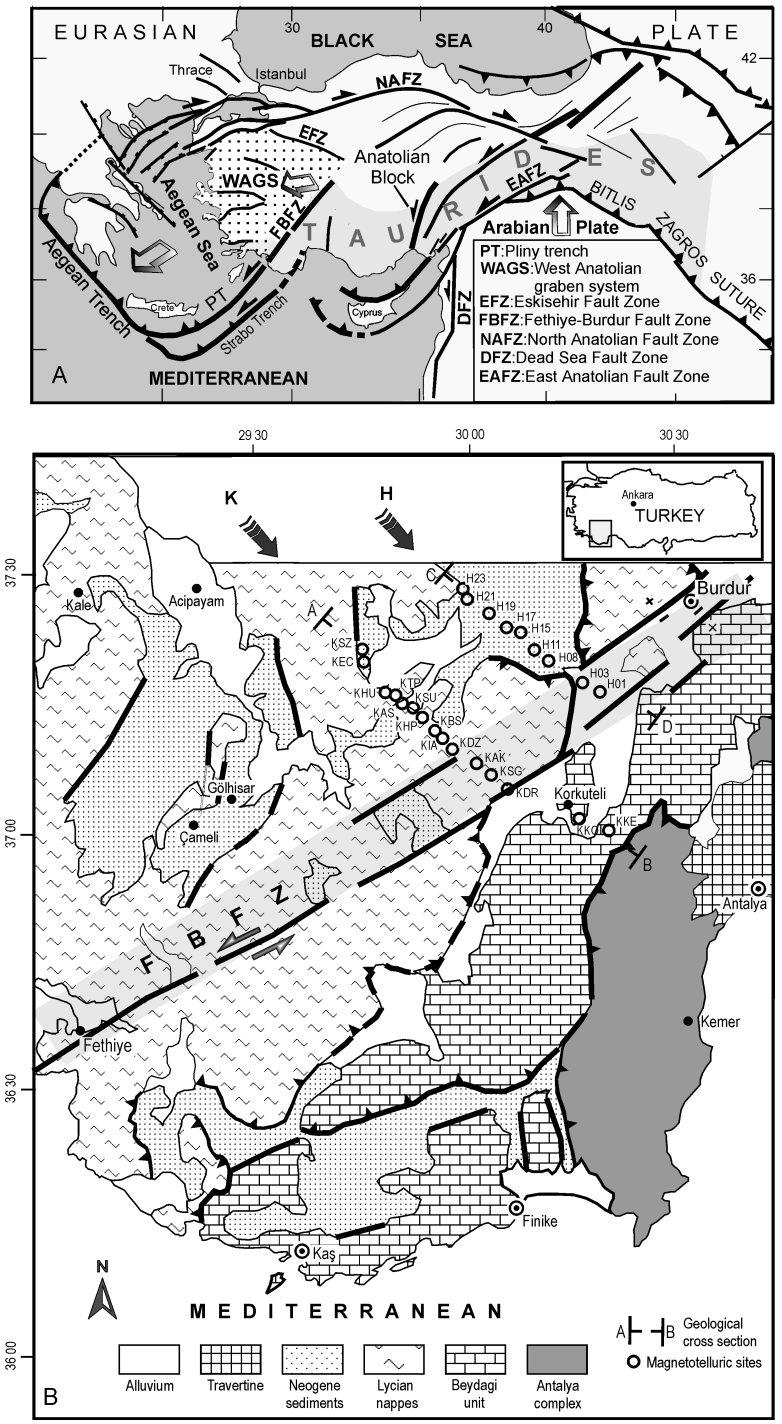

FIG. 1. A. Main tectonic elements of Anatolia and the Mediterranean region. Arrows show plate motion directions. B. Magnetotelluric site locations (circles) along profile K and profile H and tectonic map of western Turkey (modified after MTA, 1964).

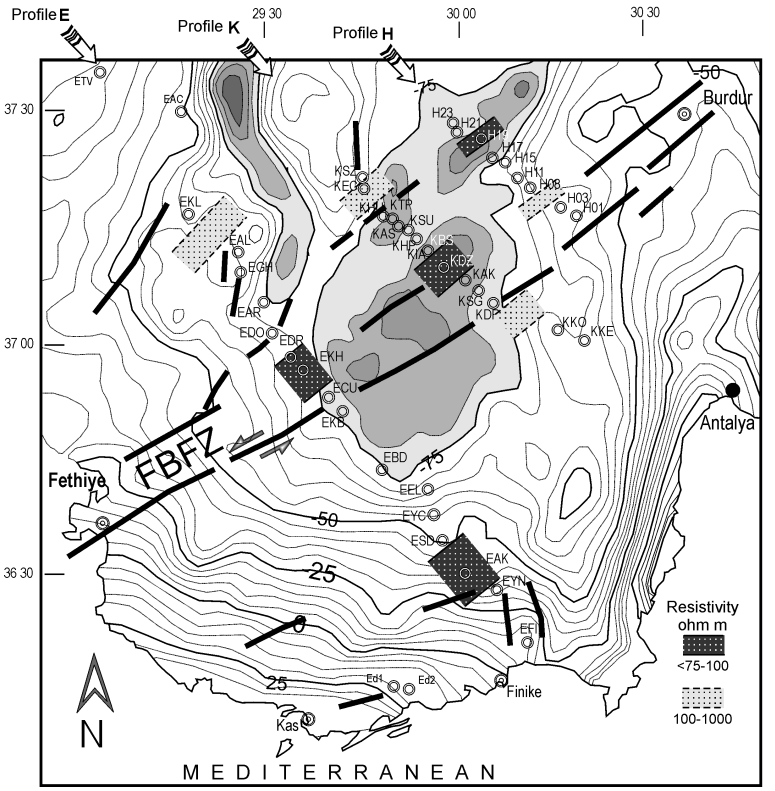

FIG. 2. Bouguer gravity map of the region (after MTA, 1999), showing the Fethiye–Burdur fault zone (FBFZ) and MT site locations. Small dotted rectangles show the projections of vertical conductivity zones in the crust.

compressional tectonic regimes respectively (Barka and Relinger, 1997). The study area, the southwestern Taurides, is thus at the junction of the rapidly deforming west Anatolian crust and the relatively stable central Anatolian crust (Barka and Relinger, 1997; McClusky et al., 2000). The geology of the area is rather complex, with high seismicity rates.

Although deep crustal structures of northwestern and western Anatolia have been investigated by several MT studies (Gürer, 1996; Bayrak et. al., 2000; Bayrak and Nalbant, 2001; Gürer et al., 2001; Çaglar, 2001; Bayrak et al., 2004), the crustal structure of southwestern Anatolia has not been fully investigated. Imaging the crustal structure of southwestern Turkey using magnetotelluric (MT) data throws light on the crustal structure and deep continuation of fault zones in the region. Furthermore, the MT images from the region will integrate MT images along another profile (profile E), 15 km west of profile K (Gürer and Ilkişik, 1999, Gürer et al., 2002).

Our profiles cross three important tectonic units of the region: the Lycian nappes, the Fethiye–Burdur fault zone (FBFZ) described above, and the Beydagi autochthon (Fig. 1B). The Lycian nappes form a tectonic package, consisting of slices of the western Taurides metamorphic basement and overlying Mesozoic platform carbonates, together with the dismembered ophiolite and volcanic-sedimentary units that form the uppermost nappe (Yilmaz et al., 2000). The FBFZ is seismically well defined by moderate and small earthquakes (Taymaz and Price, 1992). The Beydagi unit covers a large area in southwestern Anatolia. It is an autochthon composed mainly of platform-type limestones.

Earthquakes of magnitude greater than 2 that occurred between 1900 and 2000 within a margin of 40 km around the survey profile are presented for comparison with our georesistivity model results. We attempted to elucidate the crustal structure by the combined interpretation of the georesistivity model, the earthquake data, and the gravity data.

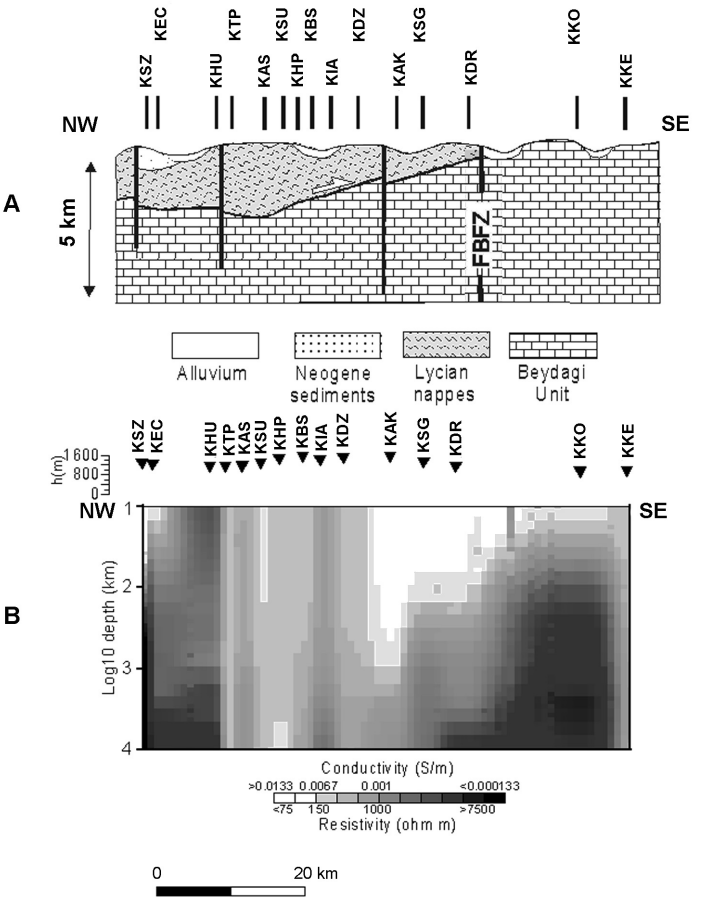

FIG. 3. A. Geological cross-section. B. The uppermost 10 km of the final georesistivity model obtained by 1-D occam inversion of the MT data along the profile K.

Data Acquisition

Figures 1B and 2 illustrate the MT site locations, together with a generalized tectonic map and the Bouguer gravity map (MTA, 1999) of the study area. These MT measurements were made along two parallel NW-SE profiles at 24 locations across southwestern Turkey (15 along profile K and 9 along profile H) by Ilkişik (1986). The average distance between the MT stations is about 4 km (Fig. 2) and the frequency range is 0.0014–6 Hz. The MT data were obtained with Geotronics MT equipment. For each site, five components of MT field (H_X, H_Y, H_Z, E_X, E_Y) were recorded. The horizontal electric and magnetic field components were measured in NW-SE and NE-SW directions with a cross-shaped configuration.

Inversion

One and two-dimensional inversions of the MT data set were undertaken using the 1-D Occam (Constable et al., 1987) and 2-D Mackie codes (Mackie et al., 1997; Rodi and Mackie, 2001) and performed on 24 MT sites. The spread of the data was for about 65 km and 36 km for profile K and profile H, respectively. We used "transverse electric" (TE) and "transverse magnetic" (TM) data for 2-D inversion and TE data for 1-D inversion. The topography is quite smooth in contrast to the land west of the study area (Gürer, 2000). The maximum elevation difference is about 500 m and slope angles are less than 5 degrees along our profiles. These values of topography do not cause significant distortion

in the MT data (Gürer, 1995; Gürer and Ilkişik, 1997).

Errors of the apparent resistivity data were increased to decrease static-shift effects; we assumed a 15% error floor for apparent resistivity and an equivalent error floor for phase. The initial model was a 100 ohm m half space. The final 1-D and 2-D resistivity models have an RMS misfit of 1 and 1.5 for profile K, respectively. The georesistivity model after 1-D inversion is shown in Figure 3B along profile K. The final two-dimensional model was determined by comparing MT parameters calculated from model with estimates provided by the field data. Figures 4 and 5 show comparisons between actual field data and best-fit model response in resistivity-phase curves and in pseudosections for the final 2-D model (Fig. 6B).

Similarly, 1-D and 2-D inversions of the data along Profile H (see Figs. 7B and 10B) give an RMS misfit of 1 and 1.6. A comparison between the model response and actual field data as resistivity and phase curves for Profile H is illustrated in Figure 8. Typical field and synthetic pseudosections from the two-dimensional model are also shown in Figure 9 for profile H. Along these two profiles, the actual data fits with the field data in terms of both apparent resistivity and phase.

Discussion

Figures 3A and 3B show the geological cross-section and 1-D georesistivity model after occam inversion along profile K. 1-D inversion of the data gives detailed and quite reliable images of the almost horizontally stratified near-surface units. Figure 3B shows the shallow part (up to 10 km depth) of the 1-D georesistivity model in order to image shallow geological structures in detail, which enables us to correlate the observed lithological and structural features in Figure 3A. Actual field data in TM and TE modes are illustrated in Figures 4 and 5 in graphical and cross-sectional forms, with the best fit 2-D model responses for profile K. Figures 6A and 6B show the subsurface conductance to 80 km depth and the final 2-D georesistivity model along profile K. The hypocentral distribution of the earthquakes occurring along the same profile is illustrated in Figure 6c.

In the same way, Figures 7A and 7B show the geological cross section and 1-D georesistivity model after occam inversion along profile H. Figures 8 and 9 represent actual field data, together with the best-fit 2-D model response. Figures 10A, 10B, and 10C show the conductance to 80 km depth, the final 2-D georesistivity model, and earthquake hypocenters along profile H.

In the georesistivity models (Figures 3B, 6B, 7B, 10B), young sediments deposited in basins are represented by low resistivity values (<75 ohm m). The Lycian nappes with their fractured and claystone-interbedded carbonates and weathered ophiolites appear as a low-resistivity zone (80 ohm m) on the geoelectrical models.

Profile K

Profile K crosses three important tectonic units of the region: the Lycian nappes, the Fethiye–Burdur fault zone, and the Beydagi unit, (Fig. 1B). The geological cross-section and the 1-D electrical resistivity image of the subsurface are shown in Figures 3A and 3B. Figures 4 and 5 show the observed field data together with the best fit 2-D model response. Figures 6A and 6B show the conductance to 80 km depth and 2-D electrical resistivity image from the surface to this depth.

In Figures 3B and 6B the area between sites KHU and KSG indicates that the conductive units (~ 80 ohm m) of the Lycian nappes (at the depth of 0.5–4 km) consists chiefly of sediments. According to the combined examination of 1-D and 2-D georesistivity models (Figs. 3B and 6B), the thickness of the Lycian nappes is ~3.5–4 km between sites KHU and KAK, decreasing to 0.5–1 km toward the southeast, at site KSG. A higher-resistivity anomaly (~ 500 ohm m) is present between sites KBS and KDZ, interrupting the continuity of the 3.5–4 km thickness of the Lycian nappes, where the thickness of the conductive nappes decreases to 0.5–1 km. The crustal conductance (the summation of the conductivity and thickness products from the surface to the investigation depth) is generally greater than 1000 S in the northwest between sites KSZ and KAK. The conductive lower crust is thicker and more conductive, and the resistive upper crust is relatively thinner and less resistive in this part of the profile. Between these sites, the uppermost sediments are also thicker (Fig. 6A).

In contrast, in the southwestern part of the profile between sites KSG and KKE, the conductivity and thickness of the lower crust decrease considerably, and the resistive upper crust becomes thicker and more resistive. As a result, the total crustal conductance in this part of the section decreases below 1000 S. The upper mantle is more resistive and

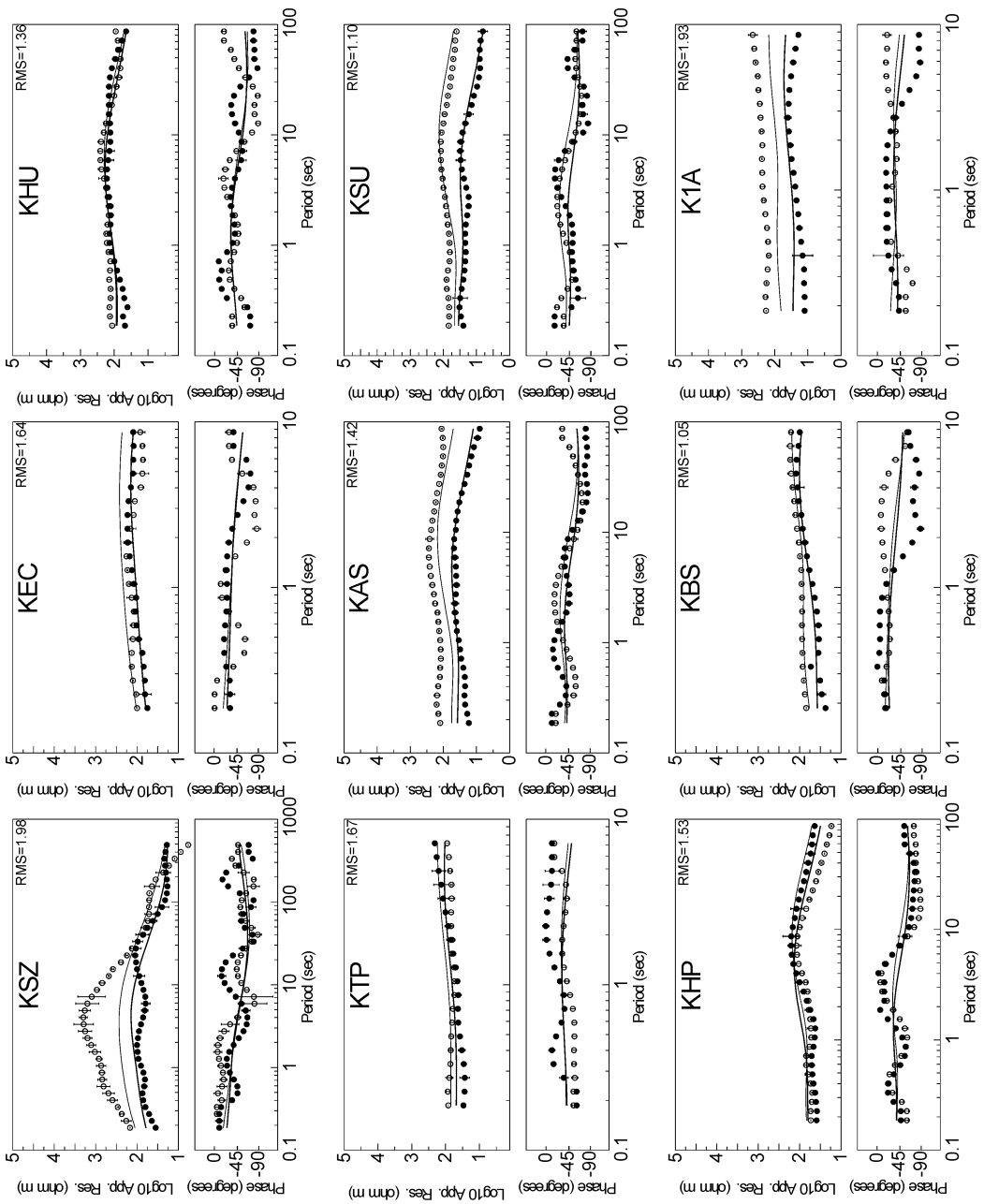
KSZ
RMS=1.98
KEC
RMS=1.64
KHU
RMS=1.36
KTP
RMS=1.67
KAS
RMS=1.42
KSU
RMS=1.10
KHP
RMS=1.53
KBS
RMS=1.05
K1A
RMS=1.93
Log10 App. Res. (ohm m)
Phase (degrees)
Period (sec)

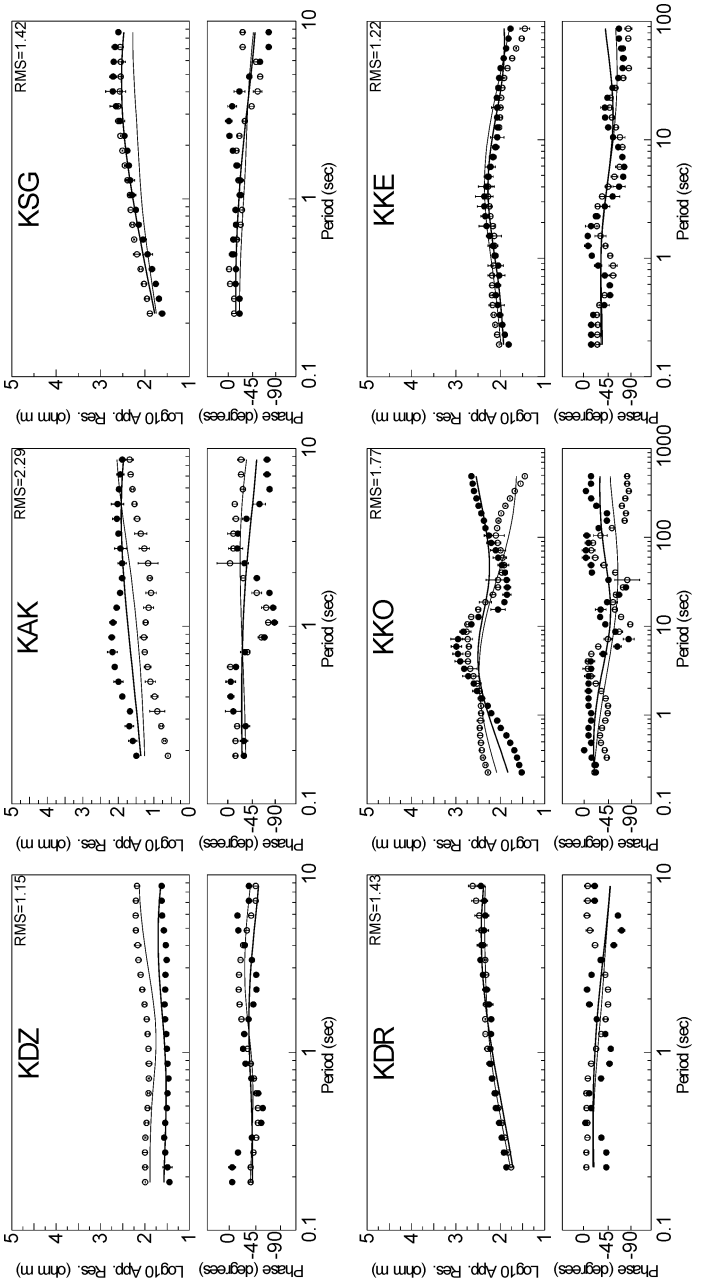

FIG. 4. A comparison of the 2-D TM response (filled circles) and TE response (open circles). MT data with the model responses (TM dense and TE light solid lines) from the model are depicted in Figure 6B for profile K.

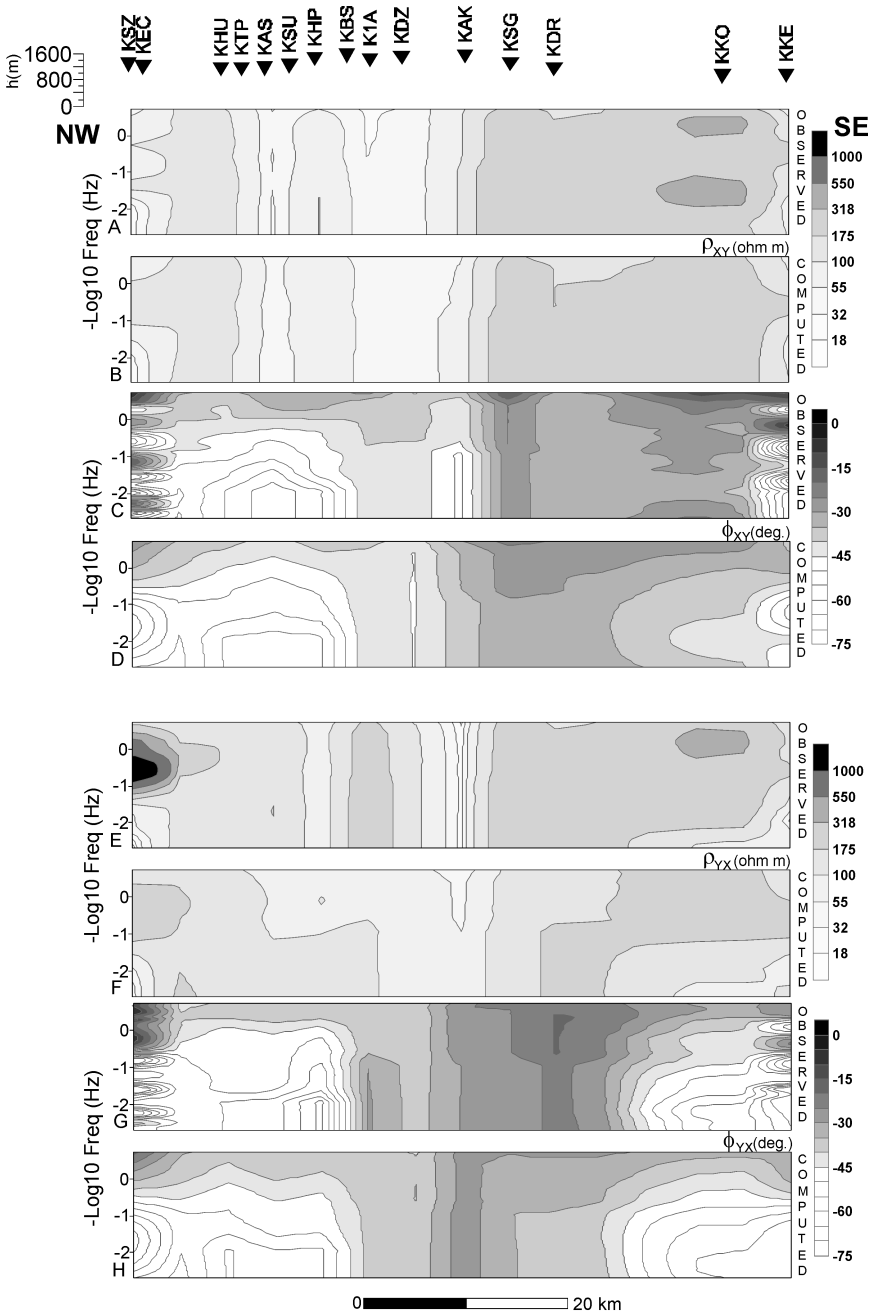

FIG. 5. Pseudosections of the MT (A) resistivity and (C) phase data along profile K comparing synthetic (B) resistivity and (D) phase data from the two-dimensional model for TM mode (ρ_{XY}, ϕ_{XY}) and pseudosections of the MT (E) resistivity and (G) phase data along profile K comparing synthetic (F) resistivity and (H) phase data from the two-dimensional model for TE mode (ρ_{YX}, ϕ_{YX}).

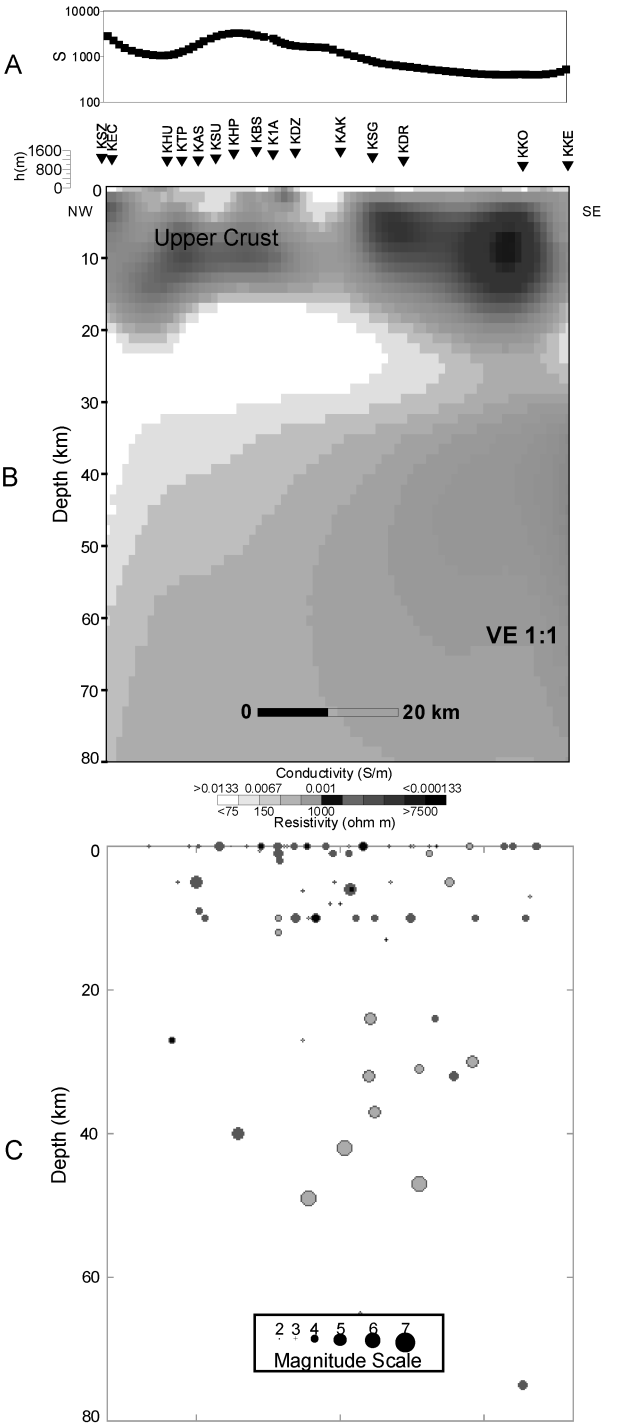

FIG. 6. A. The subsurface conductance to 80 km depth. B. Final georesistivity model obtained by 2-D inversion modelling of the MT data that is sensitive to resistivity structures to 80 km on a 1:1 exaggeration of the figure. C. Hypocentral distribution of earthquakes occurring along profile K.

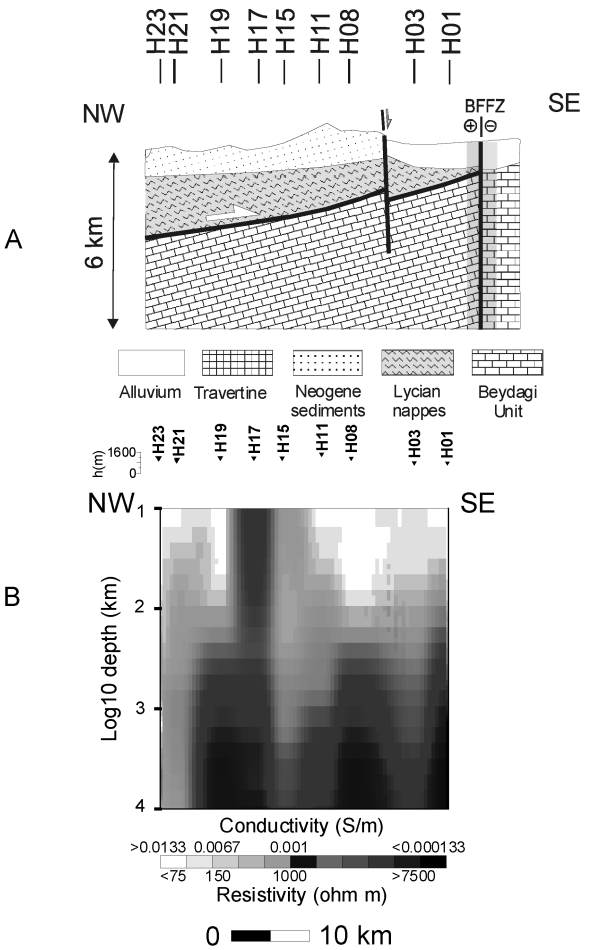

FIG. 7. A. Geological cross-section. B. The uppermost 10 km of final georesistivity model obtained by 1-D occam inversion of the MT data along profile H.

closer to the surface here. This contributes to the decrease in the total conductance in this section. Beneath the Lycian nappes, a highly resistive zone (~1000 ohm m) exists. This resistive zone may be inferred to be the Menderes Massif, which forms the basement of West Anatolian grabens (Fig. 3B).

The 2-D georesistivity model (Fig. 6B) shows some relatively conductive vertical boundaries that cut the resistive upper crust. One of these conductive (~100 ohm m) zones extending to the lower crust is identified between sites KDZ and KAK around a branch of the FBFZ (Fig. 1B). It separates the resistive upper crust into two main zones. The upper crustal zone lying to the southeast of KAK is more resistive and thicker (~500–7500 ohm m, ~ 20 km) than the northwestern zone (~500-1000 ohm m, ~14 km). The southern zone is also separated into two highly resistive cores around site KDR, which is situated on another branch of the FBFZ. It is well known that active tectonic regimes can create highly deformed fluid-bearing conductive zones in the crust (Shankland and Ander, 1983). The vertical conductive zones in the crust in southwest Anatolia are possibly created by the tectonic activity of the FBFZ.

The two-dimensional resistivity model (Fig. 6B) also successfully discriminates the brittle upper (>500 ohm m) and viscoelastic conductive lower crust (<75 ohm m) and lithospheric upper mantle. The lower crust/mantle boundary in southwest

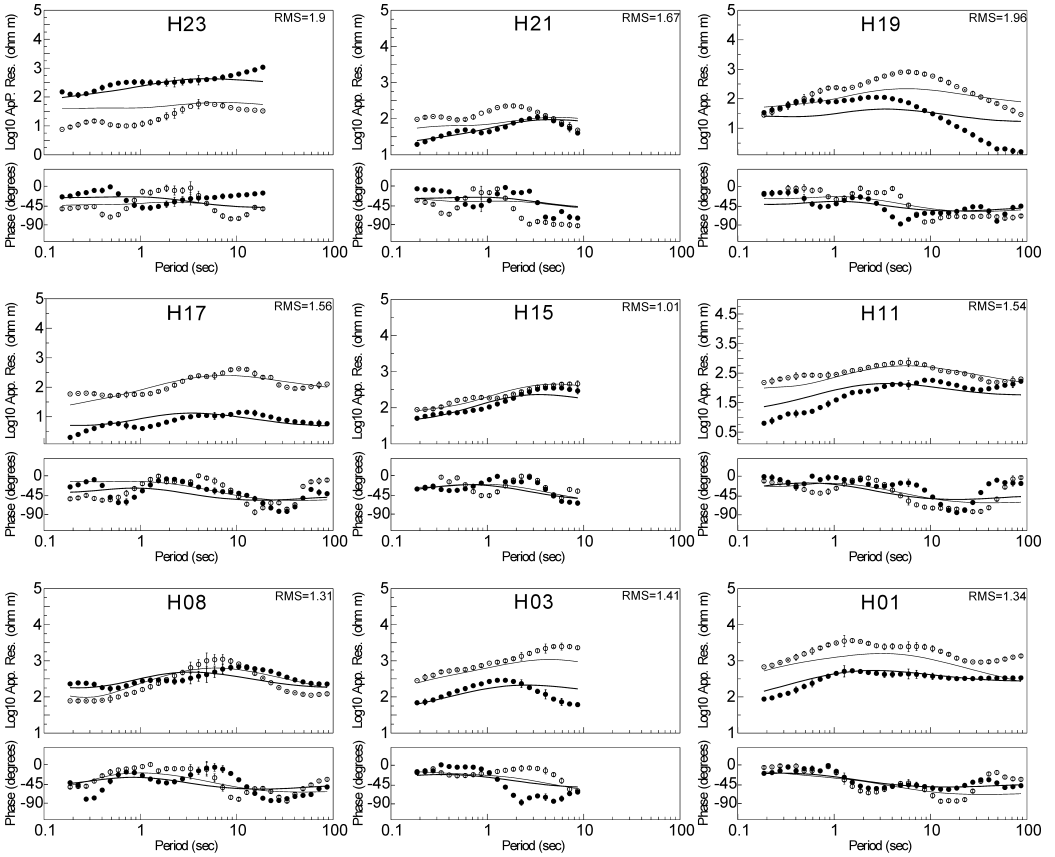

FIG. 8. A comparison of the 2-D TM response (darkened circles) and TE response (open circles) MT data with the model responses (TM dense and TE light solid lines) from Figure 10B for profile H.

Anatolia has an undulating topography along profile K, as also exists in western Anatolia (Bayrak and Nalbant, 2001; Gürer et al., 2001), with a varying total crustal thickness (from 25 to 42 km). The depth to the top of a conductive layer and the conductance of the layer are well constrained by the MT data (Li et al., 2003). In the northernmost part of the 2-D model section in Figure 6B, the top of the conductive lower crust is at its deepest level (around 23 km) and the total crustal thickness is about 42 km. The depth from the surface to the lower crust decreases from 23 to 16 km at site KHU. It remains more or less constant along the profile to the town of Düzyurt (KDZ), and increases to 20 km at site KAK in the southeast of the profile. The crust-upper mantle boundary decreases from 42 km in the northwest to 30 km in the center of the profile and 25 km in the southeast of the section.

The resistive upper crustal zone in the MT model shows a very good correlation with the hypocentral distribution of earthquakes occurring within the 40 km wide zone along our profile (Fig. 6C). A similar relation between seismically active zones and resistive cores was also observed in western Turkey (Bayrak and Nalbant, 2001; Tank et al., 2003; Bayrak et al., 2004). We also determined that the resistivity in the upper mantle is not homogeneous along the MT profile. It varies from ~80 ohm m in the northwest to ~250 ohm m at the southeastern end of the profile. The conductive upper mantle (80 ohm m) to the northwest of the profile has the same resistivity value as the viscoelastic upper mantle in western Anatolia (Bayrak and Nalbant, 2001). This low-resistivity zone may denote an anomalous region within the resistive upper mantle that coincides with the low gravity anomaly in Figure 2. This

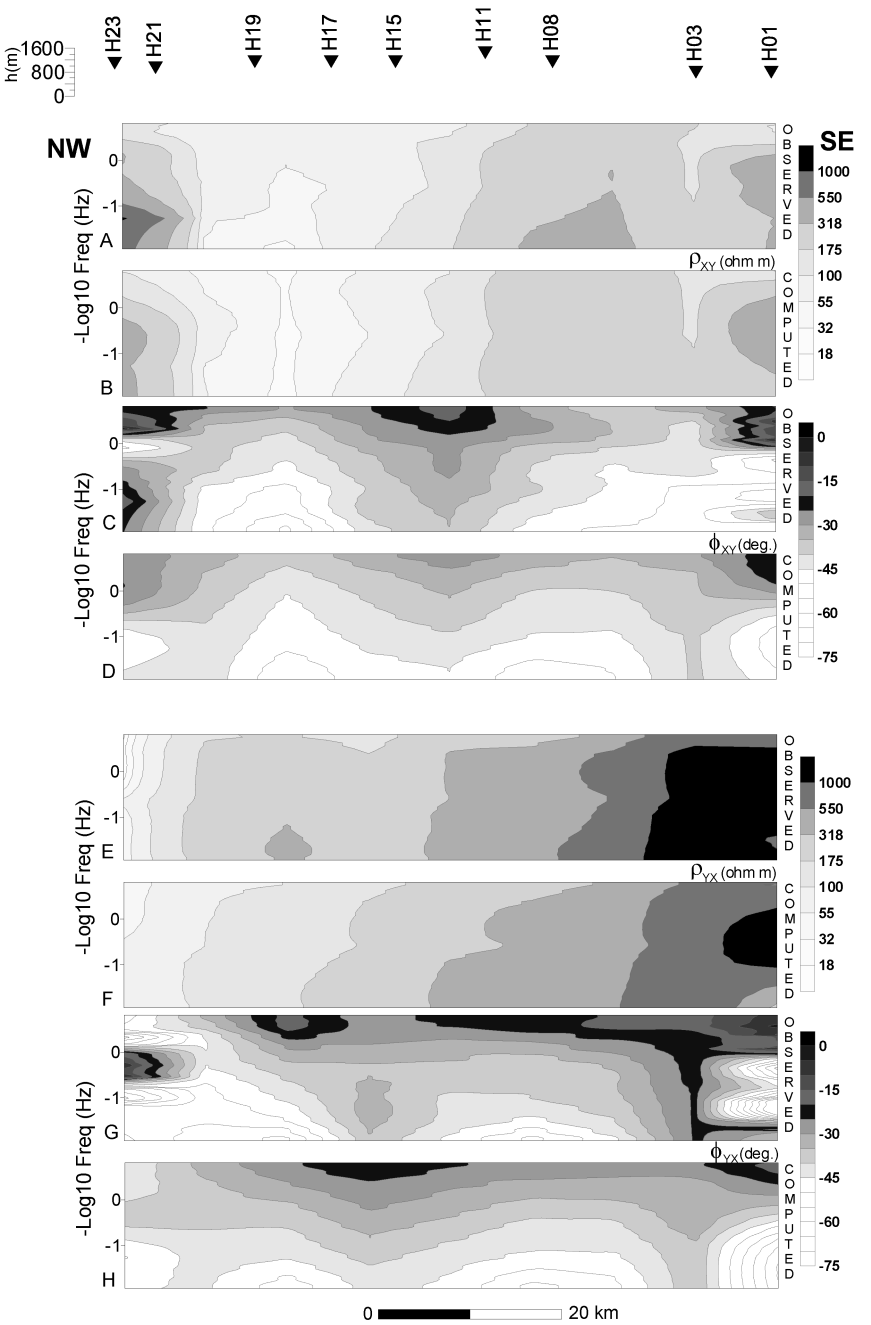

FIG. 9. Pseudosections of the MT (A) resistivity and (C) phase data along profile H comparing synthetic (B) resistivity and (D) phase data from the two-dimensional model for TM mode (ρ_{XY}, ϕ_{XY}) and pseudosections of the MT (E) resistivity and (G) phase data along profile H comparing synthetic (F) resistivity and (H) phase data from the two-dimensional model for TE mode (ρ_{YX}, ϕ_{YX}).

TABLE 1. Comparison of Heat Flow Values of West and Southwest Anatolia

Region	Location	Longitude,°	Latitude, °	Heat flow, mW/m^2
West Anatolia	Denizköy	26.85000	38.92916	109
	Haliller	28.28333	38.16250	128
	Çeşni	28.47500	38.33333	278.4
	Çataloluk	28.49167	38.85833	117.8
SW Anatolia	Bayir	28.20000	36.68333	65.9
	Balat	27.25417	37.48333	19.5
	Tekeler	27.78333	37.51667	60.1
	Kuyucak	28.26667	37.06250	43.4

Source: Ilkişic et al., 1997.

conductive mantle zone therefore warrants examination by further measurements in the region. However, there is a resistive upper mantle zone (~250 ohm m), in the southeast of profile K and along profile E (Gürer et al., 2002) in Figure 2. This value of resistivity indicates the upper mantle has lithospheric character (Jones, 1999). An earthquake occurrence region in the upper mantle coincides with this higher resistivity zone. The low gravity anomaly between sites KHU-KDR (Fig. 2), matches the relatively lower resistivity (~80 ohm m) zone in the mantle, whereas the high-resistivity mantle zone coincides with the higher Bouguer gravity anomaly. This correlation implies that earthquakes occur where the resistivity and the density are highest in the upper crust and the lithospheric mantle. This is as expected, inasmuch as rocks that are dense and electrically resistive (>250 ohm m) are probably mechanically strong enough to permit sufficient stress to accumulate for earthquakes to occur.

Our georesistivity model along profile K and the pattern of earthquake distribution in the mantle may also indicate that the mantle is separated into two parts, having different physical conditions around site KDZ. Another study (Gök et al., 2000) on Sn wave propagation, which is sensitive to the rheology of the mantle, supports our geoelectrical (MT) models in southwest Anatolia, as do models by Bayrak and Nalbant (2001) and Gürer et al. (2001) in west Anatolia. This study shows that Sn wave propagation in the mantle is attenuated in west Anatolia, denoting the presence of asthenospheric upper mantle. Meanwhile, an efficient Sn wave propagation observed in southwest Anatolia is an indication of the brittle lithospheric upper mantle in the region. Another finding by Ilkişik et al. (1997), supporting the idea that the asthonospheric upper mantle is not present in southwestern Anatolia is the very low heat flow values of the region (~ 40 mWm^{-2}) in contrast to west Anatolia (>100 mWm^{-2}) (Ilkişik et al., 1997; Gürer et al., 2001). Some typical heat flow values from west and southwest Anatolia are shown in Table 1.

Profile H

Profile H is parallel to profile K and crosses a branch of the FBFZ and Tefenni Tertiary basin 36 km long, encompassing nine MT sites. Figures 7A and 7B show the geological cross section along profile H, and the 1-D georesistivity model up to 10 km depth after occam inversion. These relatively shallow geoelectrical structures correlate with the lithological and structural features in the geological cross-section along the profile, (Fig. 7A). 1-D inversion of the data (Fig. 7B) gives the thickness of the shallow and practically horizontally stratified Tertiary sediments with very low resistivities (<75 ohm m). The sediment thickness varies from 0.1 km in the southeast to 1 km in the northwest. The basin is situated in the southwest end of the Lycian nappes and the moderately resistive zone (>500 ohm m) beneath the conductive sediments may reflect the presence of carbonates of the Beydagi autochthon. The depth to this resistive basement starts from 500 m and it has an undulating character.

Figures 8 and 9 show the comparison of the best fit 2-D model response and actual field data, the resistivity and phase curves. Figure 10A illustrates

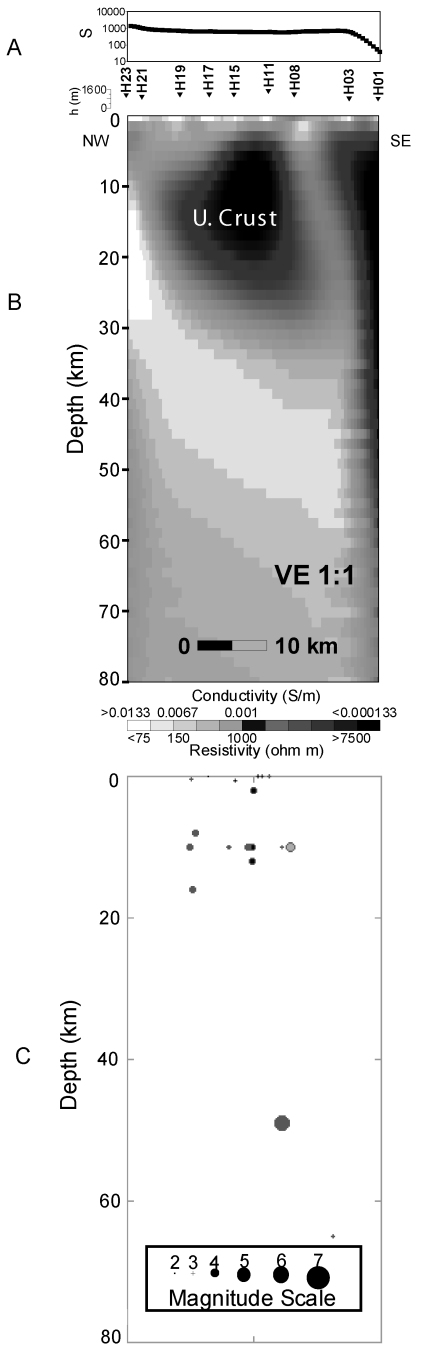

FIG. 10. A. The subsurface conductance to 80 km depth. B. Final resistivity model obtained by 2-D inversion modeling of the MT data that is sensitive to resistivity structures to 80 km on a 1:1 exaggeration on the figure (CLC, conductive lower crust). C. Hypocentral distribution of the earthquakes occurring along profile H.

conductance to 80 km depth along the profile H. Figure 10B shows the 2-D georesistivity model, which was generated using 9 MT sounding sites of ρxy-ϕxy and ρyx-ϕyx data along profile H. In Figure 10B, the georesistivity model shows two relatively less resistive, vertical zones between sites H21–H19 and between H08–H03. These zones separate the upper crust into core-shaped resistors (~2000 ohm m). The conductive zone between sites H21 and H19 may be related to the sedimentary cover of the basin. The low gravity anomaly region in Figure 2 between sites H21–H19 coincides with this conductive zone. The upper-crustal resistive core has a bottom depth of 25–30 km, and the conductive lower crust (>75 ohm m) only appears in the northwest end of the section. The total crustal thickness ranges from 28 to 32 km along profile H. The conductive lower crust is closest to the surface (at 10 km) and the total crustal thickness is lowest (28 km) in the northwest end of the profile H. The upper mantle becomes highly conductive (~80 ohm m) between sites H23–H03. This conductive zone is parallel to the conductive zone in the upper mantle along profile K, and coincides with the low gravity anomaly in Figure 2.

The resistivity increases anomalously at both crustal and mantle depths around sites H03 and H01 in the southeastern end of the section. The total crustal conductance (Fig. 10A) which is stable at 1000 S along the section, suddenly decreases to ~50 S as a result. In order to understand this anomalous decrease, and sudden changes of the crustal thicknesses, the profile H would need to be extended to the southeast with the new measurement sites.

Along profiles K, H, and the profile E from Gürer et al. (2002), the vertical conductive zones separating the resistive upper crust have been projected onto the gravity map, demonstrating the main tectonic features (Fig. 2). The projections of the vertical conductive zones show a parallel alignment to the FBFZ, and the Pliny and the Strabo fault zones in the eastern Mediterranean Sea. The interpretation of the former one-dimensional modeling has also shown such an alignment of the conductive zones in the region (Ilkişik, 1991).

Conclusions

1. In this study, the MT data measured by Ilkişik (1986) at 24 locations, along two profiles (profile K and profile H), in southwestern Turkey were inverted in 1-D and 2-D. 1-D inversion for the first

few kilometers of the subsurface gives detailed images of almost horizontally stratified near-surface units. 2-D inversion of the MT data sheds light on vertical and horizontal discontinuities in the crust and the crust and upper mantle boundary. According to the MT models, the thickness of the resistive upper crust (~500–7500 ohm m) ranges from 10–20 km. The total crustal thickness varies from 23 to 42 km along both of the profiles. The variations in the thickness of the Lycian nappes along profile K are determined as 4–0.5 km from the northwest to the southeast by 1-D and 2-D inversion.

2. The electrical resistivity is strongly dependent on the physical properties of the rocks at upper mantle depths. In contrast to western Anatolia where conductive (~ 80 ohm m) viscoelastic asthonosphere is present (Bayrak and Nalbant, 2001), our MT models and the MT model of Gürer et al. (2002) show that upper mantle is generally resistive (100–500 ohm m). The only exception is the conductive upper mantle segment beneath MT sites that coincides with the low gravity zone in Figure 2. This anomalous conductive mantle zone needs to be examined by further measurements in the region. The MT findings are supported by heat flow values for western Anatolia, higher than the world average of 85 mWm^{-2}, and southwest Anatolia, much lower than the world average, at about 40–50 mWm^{-2} (Ilkişik, 1995, Ilkişik et al., 1997). The seismological results of Gök et al. (2000) also support these MT findings. Although Sn wave propagation in the mantle is inefficient in western Anatolia, it is quite efficient in southwest Anatolia. This indicates that the upper mantle has a brittle character in southwest Anatolia in contrast to west Anatolia. Secondly, inefficient Lg (crustal guided wave) propagation in southwest Anatolia (Gök et al., 2000), indicating lateral variations in the crust, correlates with vertical discontinuities in our MT models (Figs. 6B and 10B).

3. The hypocentral distribution of earthquakes occurring within the 40 km wide zone along our MT profiles (Figs. 6C and 10C) shows that seismicity is concentrated in the resistive upper crust. There are almost no earthquakes in conductive zones of the lower crust and the upper mantle. Along profile K, there is a considerable earthquake occurrence zone (between the sites of KSU-KKO) beneath the lower crust, in the resistive upper mantle. This pattern of earthquake distribution supports the idea that the upper lithospheric mantle is brittle in character in the southeast part of the profile. Moreover, the earthquake occurrence zones coincide with the sections that have the highest resistivity in the upper mantle and the upper crust. This suggests that the main macro-earthquake occurrence can be expected in regions where both tectonic activity and electrical resistivity are high in the lithosphere.

4. The combined interpretation of the Bouguer gravity map and MT georesistivity models shows that the low gravity zone in the Bouguer gravity map coincides with the low resistivity zone in the mantle (between KHU–KSG) and with some of the vertical conductive zones in the crust along the MT profiles. The vertical conductivity zones in the crust in MT models show an alignment parallel to the FBFZ, and the Pliny and the Strabo trenches in the Aegean arc, and coincide with the low gravity anomaly. These high-conductivity and low-gravity zones may be related to the highly deformed and fractured vertical discontinuities in the crust that might be the results of subduction along the Pliny and the Strabo trenches.

Acknowledgments

This study was supported by the research Fund of the University of Istanbul (BEKADEP-159/250599 and 1781/21122001) and TUBITAK (102Y054). Many thanks are extended to Dr. Mackie for allowing us to use his EM inversion program and answering our endless questions. We also are grateful to Joanna Read for assistance with English exposition.

REFERENCES

Barka, A., and Reilinger, R., 1997, Active tectonics of the Eastern Mediterranean region: Deduced from GPS, neotectonic and seismicty data: Annal di Geofisika, v. XI, p. 3.

Bayrak, M., Gürer, A., and Gürer, Ö. F., 2004, Electromagnetic imaging of the Thrace Basin and Intra-Pontide Subduction Zone, northwestern Turkey: International Geology Review, v. 46, p. 64–74.

Bayrak, M., and Nalbant, S. S., 2001, Conductive crust imaged in western Turkey by MT: Geophysical Research Letters, v. 28, p. 3521–3524.

Bayrak, M., Ilkişik, O. M., Kaya, C., and Başokur, A. T., 2000, Magnetotelluric data in western Turkey: Dimensionality analysis using Mohr circles: Journal of Geophysical Research, v. 105, p. 23391–23401.

Constable, S. C., Parker, R. L., and Constable, C. G., 1987, Occam's inversion: A practical algorithm for generating smooth models from EM sounding data: Geophysics, v. 52, p. 289–300.

Çaglar, I., 2001, Electrical resistivity structure of northwestern Anatolia and its tectonic implications for the Sakarya and Bornova zones: Physics of the Earth and Planetary Interiors, v. 28, p. 95–110.

Gök, R., Türkelli, N., Sandvol, E., Seber, D., and Barazangi, M., 2000, Regional wave propagation in Turkey and surrounding regions: Geophysics Research Letters, v. 27, p. 429–432.

Gürer, A., 1995, Manyetotellürik tepkilerdeki topografik etkilerin düzeltilmesi ve Bati Anadolu verilerine uygulanmasi. Unpubl. Ph.D, thesis, Istanbul Üniversitesi, Fen Bilimleri Enstitüsü.

_____, 1996, Deep conductivity structure of the North Anatolian fault zone and the Istanbul Sakarya zones along the Gölpazari–Akçaova profile, Northwest Anatolia: International Geology Review, v. 38, p. 727–737.

_____, 2000, Manyetotelürikte topografya düzeltmesi ve bati Toroslara uygulanmasi: Uygulamali Yerbilimleri, no. 1–4, p. 49–61 (in Turkish).

Gürer, A., Bayrak, M., and Gürer, Ö. F., 2002, Magnetotelluric images of southwest Anatolia., 1st International Symposium of Istanbul Technical University, Faculty of Mines and Earth Sciences and Engineering. May, Istanbul.

Gürer, A., and Ilkişik, O.M., 1997, The importance of topographic corrections on magnetotelluric response data from rugged regions of Anatolia: Geophysical Prospecting, v. 45, p. 111–125.

_____, 1999, Anisotropy and terrain effect on MT data from Tauride tectonic Belt (SW Turkey): Birmingham, UK, International Union of Geodesy and Geophysics.

Gürer, A., Gürer, Ö. F., Pinçe, A., Ilkişik, O. M., 2001, Conductivity structure along the Gediz graben, west Anatolia, Turkey: Tectonic implications: International Geology Review, v. 43, p. 1129–1144.

Ilkişik, O. M., 1986, Western Taurides magnetotelluric measurements and interpretation project: Istanbul, Turkey, I.T.Ü. Mining Faculty, TPAO Technical Report, 80 p. (in Turkish).

_____, 1991, Magnetotelluric investigations in the western Taurides region: Izmir, Turkey, IESCA-1991, Proceedings, p. 40–51.

_____, 1995, New heat flow data-set using silica estimator from thermal springs in western Anatolia: Tectonophysics, v. 224, p. 175–184.

Ilkişik, O. M., Yalçin, M. N, Sari, C., Okay, N., Bayrak, M., Yenigün, H., Şardar, S., and Oguz, S., 1997, Ege Bölgesinde Jeotermik Araştirmalar. Ulusal Deniz Jeolojisi ve Jeofizigi Güdümlü Projesi: Ankara, Turkey, TÜBITAK, YDABÇAG_430/G.

Jones, A. G., 1999, Imaging the continental upper mantle using electromagnetic methods: Lithos, v. 48, p. 57–80.

Kocyigit, A., 2000, Seismicity of southwest Turkey: Bati Anadolu'nun Depremselligi Simpozyumu, Izmir, p. 30-38.

Li, S., Unsworth, M. J., Booker, J. R., Wei, W., Tan, H., and Jones, A. G., 2003, Partial melt or aqueous fluid in the mid-crust of Southern Tibet?: Constraints from in-depth magnetotelluric data: Geophysical Journal International, v. 153, p. 289–304.

Mackie, R., Rieven, S., and Rodi, W., 1997, Users manual and software documentation for two-dimensional inversion of magnetotelluric data: San Francisco, CA, GSY-USA Inc., 14 p.

McClusky, S., Balassanian, S., Barka, A., Demir, C., Georgiev, I., Hamburg, M., Hurst, K., Kahle, H., Kastens, K., Kekelidze, G., King, R., Kotzev, V., Lenk, O., Mahmoud, S., Mishin, A., Nadariya, M., Ouzounis, A., Paradissis, D., Peter, Y., Prilepin, M., Reilinger, R., Sanli, I., Seeger, H., Tealeb, A., Toksoz, M. N., and Veis, G., 2000, Global positioning system constraints on plate kinematics and dynamics in the eastern Mediterranean and Caucasus: Journal of Geophysical Research, v. 105, p. 5695–5720.

McKenzie, D., 1978, Active tectonics of Alpine-Himalayan belt: The Aegean Sea and surrounding regions: Geophysical Journal of the Royal Astronomical Society, v. 55, p. 217–254.

MTA, 1964, Geological map of Turkey, scale 1:500,000, Denizli sheet: Ankara, Turkey, Instute of Mineral Research and Exploration.

_____, 1999, Bouguer anomaly map of Turkey: Ankara, Turkey, General Directorate of Mineral Research and Exploration, Geophysics department.

Rodi, W., and Mackie, L. R., 2001, Nonlinear conjugate gradients algorithm for 2-D magnetotelluric inversion: Geophysics, v. 66, p. 174–187.

Shankland, J. T., and Ander, M. E., 1983, Electrical conductivity, temperatures and fluids in the lower crust: Journal of Geophysical Research, v. 88, B11, p. 9475–9484.

Tank, S. B., Honkura, Y., Ogawa, Y., Oshiman, N., Tunçer, M. K., Matsushima M., Çelik, C., Tolak, E., Işikara, A. M., 2003, Resisitivity structure in the western part of the fault rapture zone associated with the 1999 Izmit earthquake and its seismogenic implications: Earth, Planets, Space, v. 55,437–55,442.

Taymaz, T., and Price, S., 1992, The 1971 May 12 Burdur earthquake sequence, SW Turkey: A synthesis of seismological and geological observations: Geophysical Journal International, v. 108, p. 589–603.

Temiz, H., Poisson, A., Andrieux, J., and Barka, A., 1997, Kinematics of the Plio-Quaternary Burdur–Dinar cross fault system in SW Anatolia (Turkey): Annales Tectonicae, v. XI, nos. 1–2, p. 102–113.

Yagmurlu, F., 2000, Seismotectonic features of the Burdur fault: Bati Anadolu'nun Depremselligi Sempozyumu, Izmir, p. 143–151.

Yilmaz, Y., Genç, Ş. C., Gürer, Ö. F., Bozcu, M., Yilmaz, K., Karacik, Z., Altunkaynak, C., and Elmas, A., 2000, When did the western Anatolian grabens begin to develop?, *in* Bozkurt, E., Winchester, J. A., and Piper, J. D. A., eds., Tectonics and magmatism in Turkey and the surrounding area: Geological Society of London, Special Publication no. 173, p. 353–384.